THE JOURNAL OF PHYSICAL CHEMISTRY B

Article

pubs.acs.org/JPCB

Control of Crystal Morphology in Monodisperse Polyfluorenes by Solvent and Molecular Weight

Chengfang Liu,[†,‡] Qilin Wang,[†,‡] Hongkun Tian,[†] Jian Liu,[†,‡] Yanhou Geng,[†] and Donghang Yan*[,†]

[†]State Key Laboratory of Polymer Physics and Chemistry, Changchun Institute of Applied Chemistry, Chinese Academy of Sciences, Changchun, 130022, P. R. China

[‡]University of Chinese Academy of Sciences, Beijing, 100049, P. R. China

ABSTRACT: Different crystalline forms are obtained by simply manipulating the good/poor solvent ratio in mixed solvents of toluene/ethanol. Depending on different solvent ratios, poly(9,9-dioctylfluorene)s (PFOs) can generate a large palette of morphologies including lenticular crystals, fibrous crystals and rod-like crystals. In the crystallization process, polymer chains experience different kinetic pathways, yielding lenticular crystals in the toluene solution, rod-like crystals at a low toluene/ethanol ratio (1:1), and fibrous crystals at a high toluene/ethanol ratio (3:1). A combination of atomic force microscopy (AFM) and transmission electron microscopy (TEM) provides an opportunity to elucidate the distinctive molecular arrangements in these different crystals. Moreover, the influence of molecular weights on the crystallization of polymers has also been investigated in different crystals.

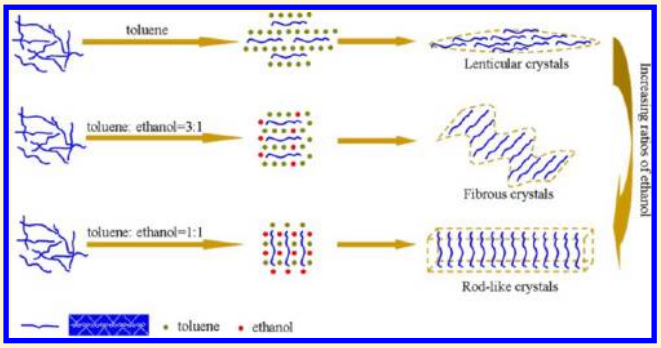

INTRODUCTION

Conjugated polymers have received wide attention as promising materials for use in thin film transistors, light-emitting diodes, and solar cells.[1−7] Since different crystalline forms of a given polymer can have significantly different solid-state properties, giving rise to variation in performance of devices,[8−11] it is imperative to gain insight into the diversity of crystalline forms available to the polymer. Thus, in many industrial contexts, great energy is exerted on the discovery, characterization, and analysis of the range of crystalline forms that can exist under different conditions,[12−24] in pursuit of establishing which specific form is optimal for a particular application.

Among various types of conjugated polymers, poly(9,9-dioctylfluorene)s (PFOs, named as F*n*) have been extensively studied due to their rich polymorphisms[19] and various applications.[25−27] It is well accepted that the increase in performance of devices has been attributed to modifications of crystalline forms and their final morphologies. Therefore, F*n* can be taken as a model system to provide a fundamental understanding about the factors on the development of crystal morphologies, further achieving outstanding optoelectronic properties. Moreover, another important parameter is the molecular weights that influence the crystallinity.[28−30] Although considerable progress in the structure of PFOs[19,20,31−37] is mainly in the form of thin films, the knowledge about the intrinsic features is still limited. Thus, it is of significance to manipulate the crystal morphologies through experimental variables such as the solvent and molecular weights to explore the molecular packing behavior in the crystal growth.[38−42]

In this work, we take a simple approach to control crystalline forms of F*n* by dissolving the sample in a certain quantity of a good solvent with different amounts of a poor solvent.[41,43] Toluene is a good solvent for F*n*, while ethanol is a poor solvent for F*n*. First, F*n* exhibits the lenticular morphology in toluene solution. Then, depending on the toluene/ethanol ratio, polymer chains experience different kinetic pathways, yielding rod-like crystals at a low toluene/ethanol ratio (1:1), and fibrous crystals at a high toluene/ethanol ratio (3:1). Furthermore, we also explore the effects of molecular weights on the morphology of polymers. Therefore, these results not only demonstrate the feasibility of controlling the morphology of crystals but also open a deep perspective for the understanding of polymer crystallization. More importantly, this work has manifested great potential to be further developed into a facile method to tune the crystal morphology according to the actual requirement in industrial application.

EXPERIMENTAL SECTION

2.1. Materials. The synthesis of monodisperse F*n* was reported previously,[44] where *n* represents the number of fluorene units. The molecular weights (M_{MS}) obtained from MALDI-TOF mass spectrometry of F16, F32, and F64 are 6220 g/mol, 12437 g/mol and 24874 g/mol, respectively. The corresponding contour length of F16, F32 and F64 are 13.3 nm, 26.6 and 53.1 nm, which are calculated according to the

Received: February 4, 2013
Revised: May 21, 2013
Published: July 2, 2013

 © 2013 American Chemical Society dx.doi.org/10.1021/jp401261u | *J. Phys. Chem. B* 2013, 117, 8880−8886

repeat distance of 0.83 nm.[32] Toluene and ethanol were purchased from Beijing Chemical Works and used without further purification.

2.2. Sample Preparation. Solutions were prepared from a ratio of good to poor solvents, denoted subsequently as A:B, where A gives the volume fraction of the good solvent, and B is the corresponding volume fraction of the poor solvent. The solution of F*n* was carried out by first dissolving the sample in toluene followed by the addition of ethanol very slowly. All the solutions have the same concentration of 0.0025 mg/mL. The substrate was put inside a cylinder container with a radius and height of 1.5 and 3.0 cm, respectively. The solution was dropped onto the glass and the container was then carefully sealed.

2.3. Characterizations. Atomic force microscopy (AFM) images were obtained using an SPA-300HV instrument with an SPI3800N controller (Seiko Instruments Inc., Japan) in tapping mode. A silicon microcantilevel (spring constant = 15 N/m, resonant frequency ≈130 kHz, Olympus, Japan) was used for the scanning.

Transmission electron microscopy (TEM) experiments were performed using a JEOL JEM-1011 with an accelerating voltage of 100 kV and selected area electron diffraction (SAED) modes. The samples for TEM were floated away from the substrate in 10% HF solution and then picked up with a copper grid. The camera length was calibrated with Au to calculate the *d*-spacing of the observed electron diffraction (ED).

RESULTS AND DISCUSSION

To highlight the correlation between the solvent, the molecular weight, and the resulting morphologies, we prepared crystals of different shapes from the mixed selective solution. The solvent was a mixture of toluene and ethanol with increasing ratios of ethanol. Measurements were done for samples of three different molecular weights (F16, F32, and F64).

3.1. Formation of Lenticular Crystals. In Figure 1, we depict the representative AFM images of lenticular crystals of F16, F32, and F64, with an average length of about 2 μm. It is illustrated that height images are measured along the cross section, where apparent changes are noted in the height profiles. Upon increment of M_{MS}, morphological changes exist and the crystals become more ill-defined for F64.

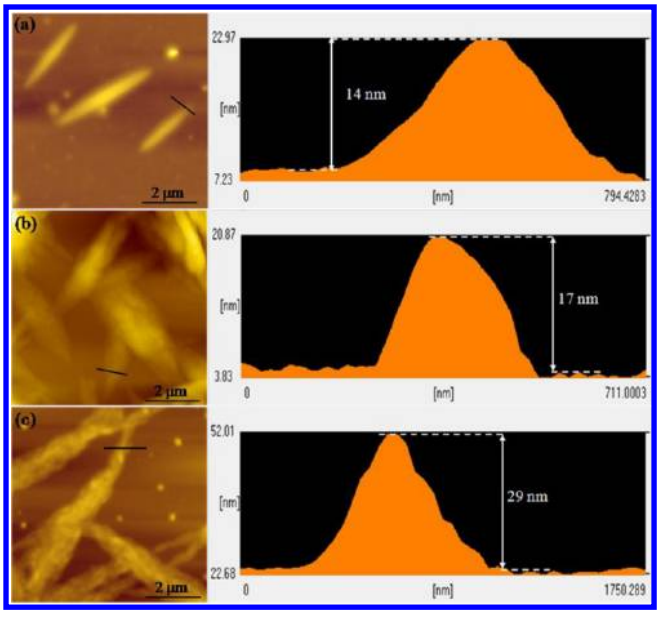

Figure 1. AFM height images and height profiles of lenticular crystals of F16 (a), F32 (b), and F64 (c).

Figure 2 shows the TEM images in bright-field (BF) mode and SAED patterns of F16, F32, and F64. By the way, the

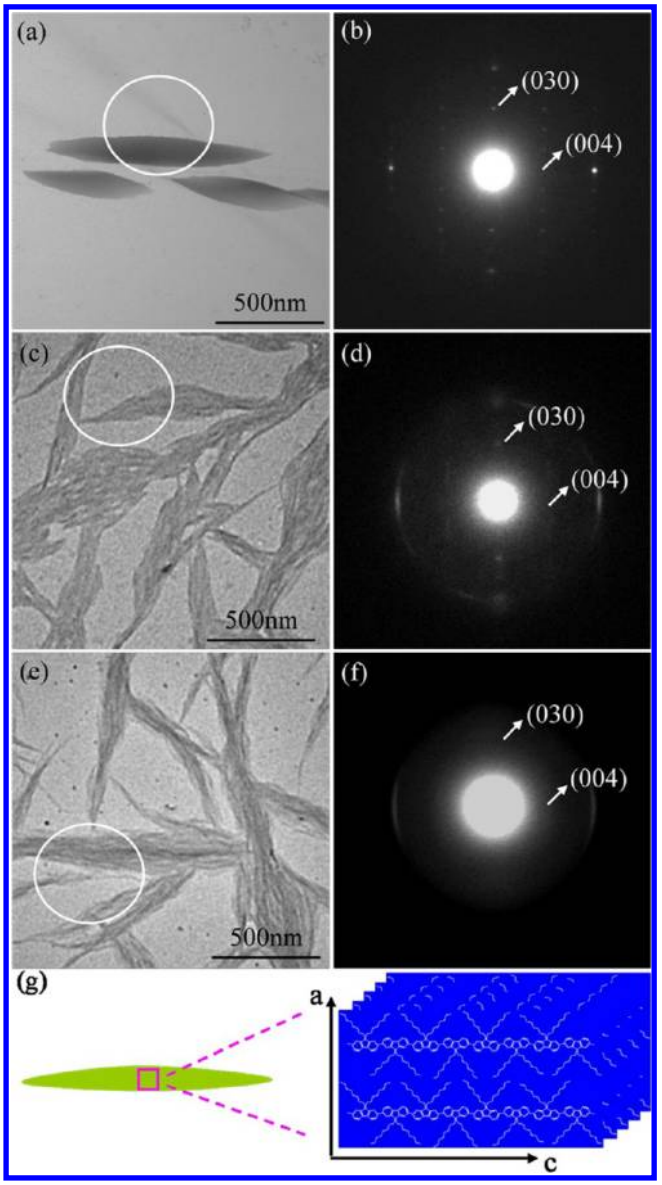

Figure 2. The TEM images and SAED patterns of crystals prepared from F16 (a and b), F32 (c and d) and F64 (e and f). (g) Simplified schematic illustrations of chain packing in the crystals.

diffraction pattern is obvious, and it will disappear with the time pass by. As shown in Figure 2b, there are two principal reflections that have been indexed as (030) and (004), the corresponding spacing being 0.70 and 0.84 nm, respectively. These values are in good agreement with the dimensions of the bc projection reported previously, which has proposed an orthorhombic unit cell with a = 1.32 nm, b = 2.10 nm, and c = 3.36 nm.[23] These observations led to the hypothesis that polymer chains in lenticular crystals assemble with the backbones parallel to the long axis of crystals and the alkyl side chains perpendicular to the substrate, as shown in Figure 2g. A similar molecular stacking motif has also been observed

dx.doi.org/10.1021/jp401261u | J. Phys. Chem. B 2013, 117, 8880−8886

for several polymers such as cyclopentadithiophene-benzothiadiazole (CDT-BTZ) copolymers,[45] thioacetate-substituted poly(para-phenylene ethynylene) (TA-PPE),[46] poly (ferrocenyldimethylsilane-block-2-vinylpyridine) (PFS-*b*-P2VP) diblock copolymers,[47] and poly3-octylthiophene (P3OT).[48] As demonstrated in our previous study, lenticular crystals from the *o*-dichlorobenzene (ODCB) solution of 0.5 mg/mL also yield spot-like diffraction,[23] and they are much larger in size than those from toluene solution. This is attributed to the larger concentration, for the concentration of the solution will change the size of the crystals.

For F32 in Figure 2d, the ED pattern is characterized by the coexistence of the (030) and (004) reflections. In the case of F64, some weaker reflections are noted, manifesting a comparatively low level of crystallinity of the sample (Figure 2f). Therefore, in the present case, the molecular packing behavior is maintained in these lenticular crystals. However, the degree of order decreases with increasing M_{MS}.

Based on the experimental data in Figure 2, sharp and intense reflections are observed for F16, while the ED pattern of F64 exhibits only a few weak reflections. Thus, one can estimate that the increase in M_{MS} leads to an overall decrease of the crystallinty of the samples demonstrated by the decrease of the intensity of the reflections in the ED pattern.

3.2. Growth of Fibrous Crystals. In order to reveal the effect of the solvent on the morphology, a definite quantity of ethanol (poor solvent) was added slowly to the toluene solution. Figure 3 shows the AFM images of fibrous crystals of

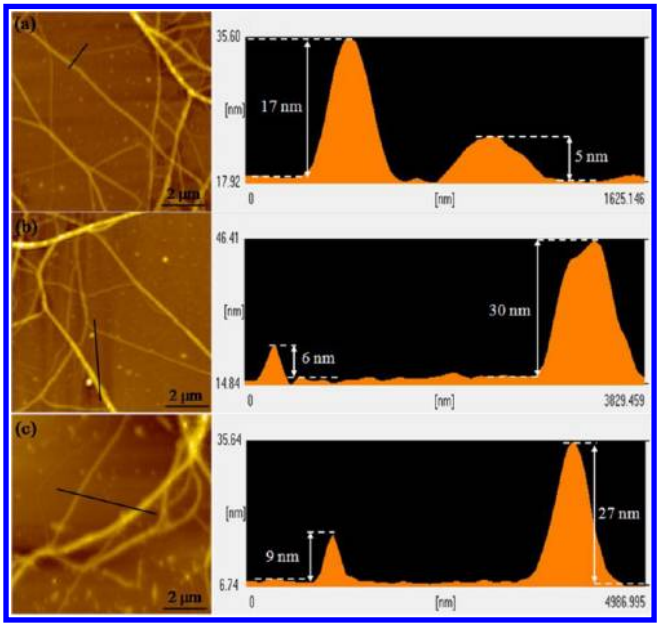

Figure 3. AFM height images and height profiles of fibrous crystals of F16 (a), F32 (b), and F64 (c).

different samples (F16, F32, and F64), which are prepared from the toluene/ethanol ratio of 3:1 solution. For each sample, they form randomly distributed fibers regardless of M_{MS}. As shown in height profiles, the variation of thicknesses in Figure 3 corresponds to thicknesses of several layers of stacked polymer chains with the side alkyl chain interdigitated with other layers. In Figure 4, we show the typical fibrous morphologies by TEM and the corresponding ED patterns for F16, F32, and F64. Fibrous crystals appear to be particularly sensitive to the

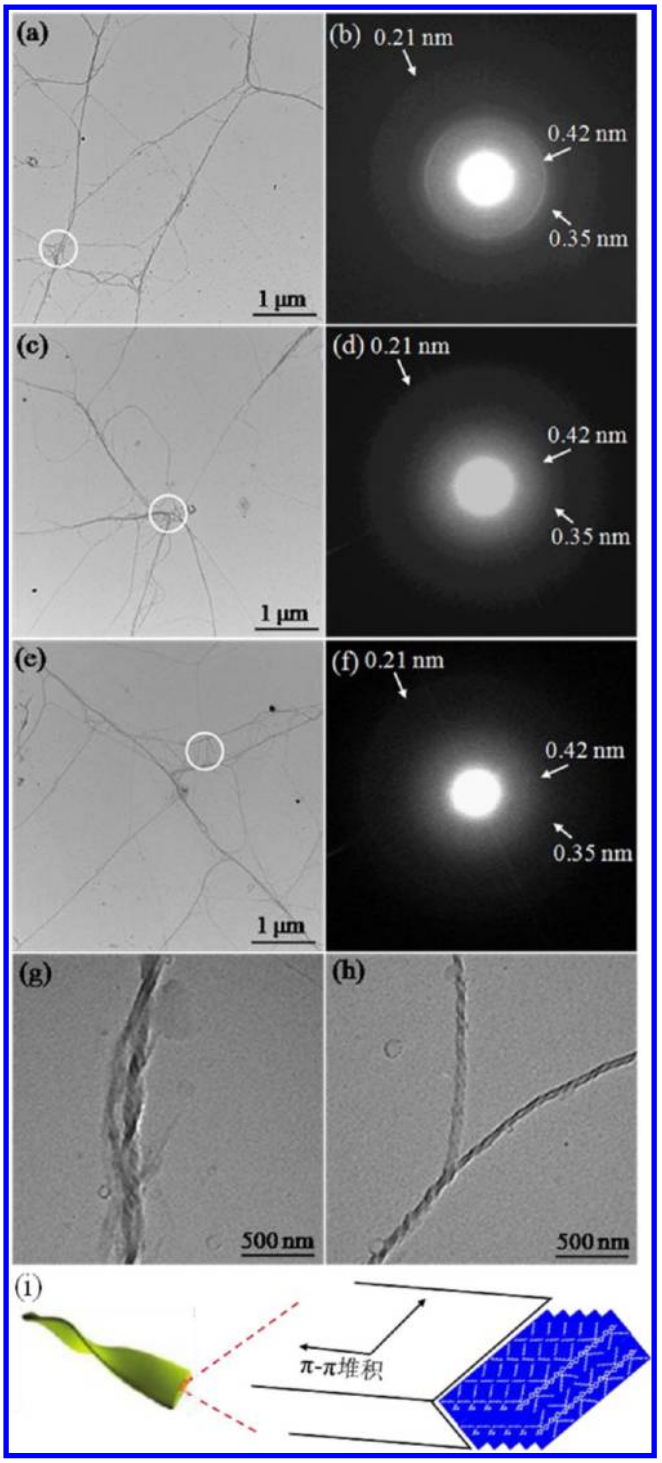

Figure 4. TEM images and SAED patterns of crystals prepared from F16 (a and b), F32 (c and d), and F64 (e and f). Magnified TEM images for clear identification of helical structures of F64 (g and h). (i) Simplified schematic illustrations of chain packing in the crystals.

electron beam, even at very low intensities. Diffraction patterns can only be obtained by using low beam intensities and working rapidly. As illustrated in Figure 4b, a repetition unit of 0.42 nm along the polymer chain direction and a repetition unit of 0.35 nm along the $\pi-\pi$ stacking direction are observed from the SAED results of F16. By a thorough analysis of the ED data, one can propose that the backbones are arranged perpendicular to the long axis of the fibers (see sketch in Figure 4i). The

dx.doi.org/10.1021/jp401261u | *J. Phys. Chem. B* 2013, 117, 8880−8886

driving force for this type of stacking is $\pi-\pi$ interactions between adjacent chains. It is observed that polymer chains studied under this condition behave in a manner similar to P3HT, which has been investigated intensively.[49]

At the same time, increasing M_{MS} leads to the weaker reflection and the lower crystallinity, as shown in Figure 4d,f. This trend can also been found in several studies of the P3HT structures. Accordingly, the effect of molecular weights on the crystalline structure is not specific to the crystallization of F*n*, but seems to be a general feature of conjugated polymers such as P3HT.[30] In large magnification, it is intriguing to note that fibers appear helical structures,[50,51] as a result of the helical twisting of the individual fibers. As shown in Figure 4g,h, helical structures still remain in F64. However, the origin of the helical twisting is complex and needs further investigation in future.

3.3. Preparation of Rod-like Crystals Composed of Lamellae. For higher amounts of ethanol, the toluene/ethanol ratio approaches 1:1, and rod-like crystals are obtained from the mixed solution. Figure 5a,b shows the typical TEM image and SAED pattern of the rod-like crystal of F16. This diffraction pattern can exist for a long time in comparison with that of lenticular crystals and fibrous crystals. The pattern shows rectangular lattice, and the *d*-spacing along the two perpendicular directions is 0.36 and 0.64 nm, indexed as (600) and (020) in terms of orthorhombic lattice parameters (a = 2.16 nm, b = 1.28 nm, and c = 3.36 nm).[22] The (hk0) reflections in SAED pattern shown in Figure 5b indicate that the electron beam goes along the [001] zone. According to the structural analysis, it is shown that backbones of F16 chains within the crystals pack vertical to the substrate with their side chains parallel to the substrate and along the crystal growth direction. In this case, interaction of alkyl side chains may be the dominant driving force for the growth of single crystals. Furthermore, the SAED patterns of F32 and F64 (Figure 5d,f) are the same as that of F16, demonstrating all three samples have the same packing mode in the crystals. Alternatively, the schematic illustration is depicted in Figure 5g.

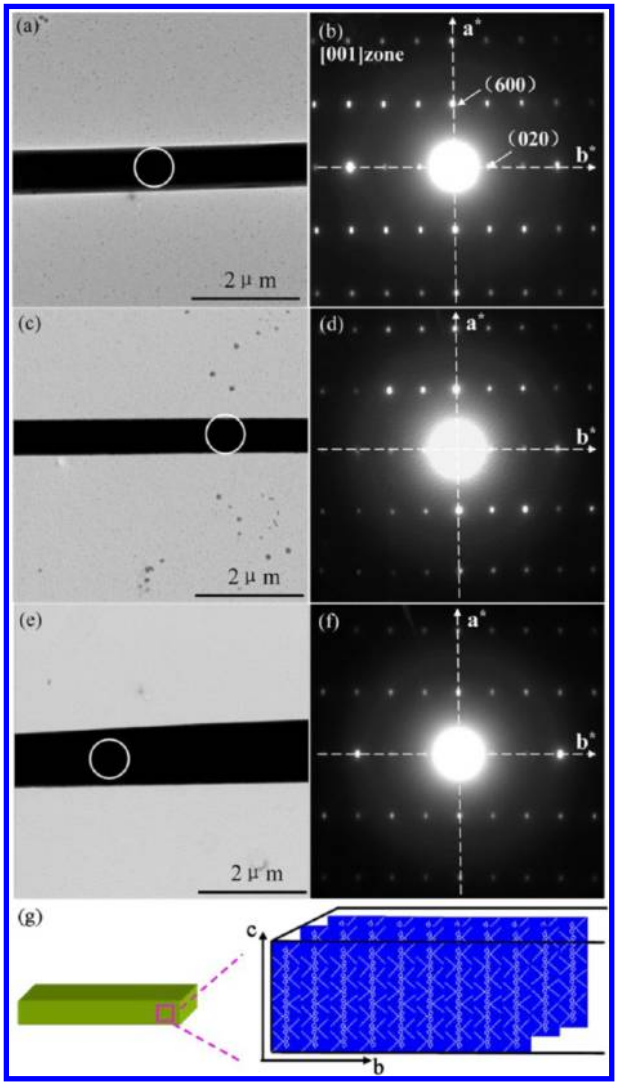

Figure 5. The TEM images and SAED patterns of crystals prepared from F16 (a and b), F32 (c and d), and F64 (e and f). (g) Simplified schematic illustrations of chain packing in rod-like crystals.

The further confirmation of the polymer chain stacking mode is provided by AFM studies. As a matter of fact, the rod-like crystals demonstrate lamellar structures, whose thicknesses correspond to their extended chain lengths. Due to the detailed investigation about this part in our previous study,[22,43] we now mainly focus on the crystals in their early growth stage and an extensive investigation at larger thicknesses is omitted. Figure 6

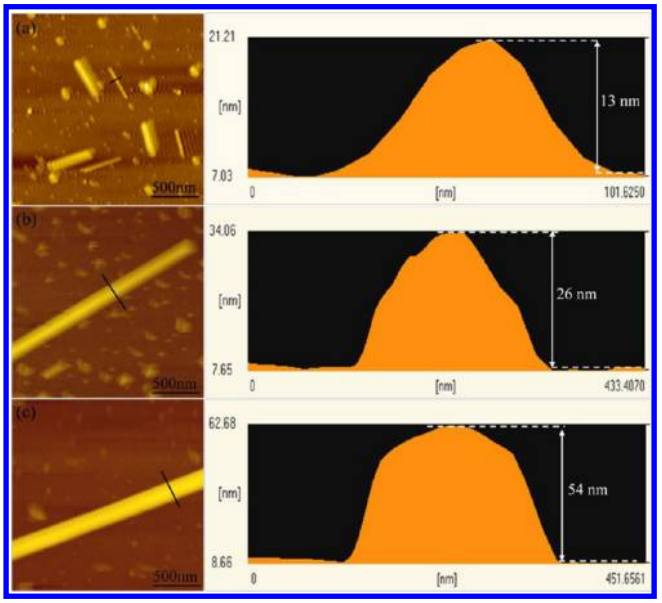

Figure 6. AFM height images and height profiles of crystals of F16 (a), F32 (b), and F64 (c) in their early stage, respectively.

shows the AFM characterization of crystals prepared from F16, F32, and F64, respectively. These AFM images exhibit the similar rod-like morphologies as observed by TEM. As shown in Figure 6a, the height profile of F16 crystals demonstrates the thickness of 13 nm. The calculated extended chain length according to the actual molecular weight (M_{MS}) of F16 is about 13.3 nm, which accords well with the thickness observed from AFM. For F32 (Figure 6b), the corresponding thickness (26 nm) is approximately close to the extended chain length of F32 (26.6 nm). The thickness of crystals of F64 in their infancy demonstrates the characteristic value of 54 nm, identical to the extended chain length of F32 (53.1 nm), which can be clearly revealed by the height profile as depicted in Figure 6c. In a word, these rod-like crystals are in their early stage, whose thicknesses correspond to one layer. Moreover, other crystals

dx.doi.org/10.1021/jp401261u | J. Phys. Chem. B 2013, 117, 8880−8886

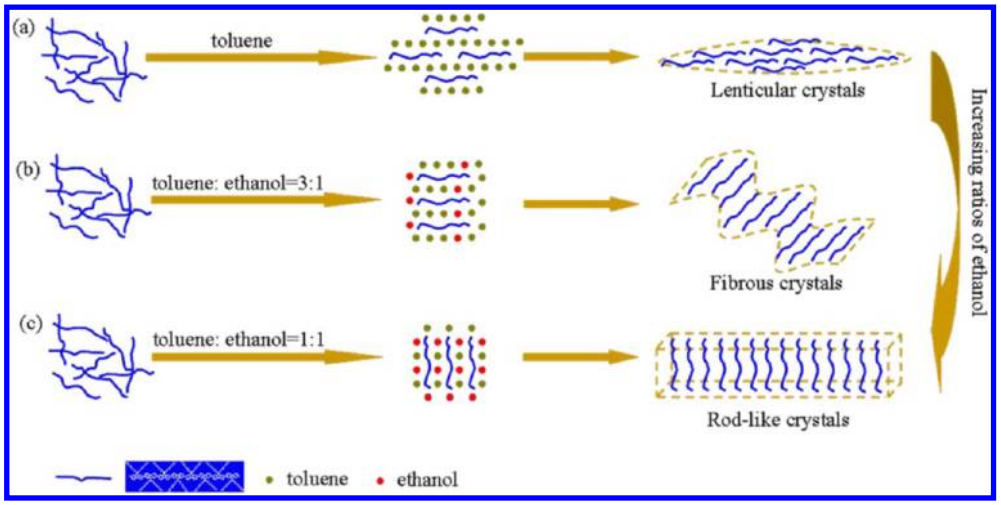

Figure 7. The hypothesized growth mechanism for the formation of lenticular crystals (a), fibrous crystals (b), and rod-like crystals (c).

on the substrate possess different thicknesses, which fit the integral fractions of the chain length, thus indicating that crystals comprise several layers.

In this way, we can speculate that the thicknesses of crystals are proportional to the chain lengths with the molecular weight (M_{MS}) increment, suggesting F*n* molecules are packed normal to the lamella with extended-chain conformation. It is noteworthy to mention that F64 still remaind extended even when the chain length is as long as 53 nm. Furthermore, experimental data indicate the molecular weight has a negligible effect on the crystallinity due to the special molecular packing. On the basis of the previous study, rod-like crystals in which chains adopt perpendicular alignment demonstrate better thermal stability than lenticular crystals and fibrous crystals.[23,43] Therefore, compared with other crystals, the rod-like crystal belongs to a different crystalline phase. In this case, the molecular weight has little influence on the morphology of crystals.

By further increasing the amounts of ethanol, the toluene/ethanol ratio reaches 1:3, and only aggregates of no specific shapes are obtained from solution.

3.4. Mechanism of the Formation of Various Crystals.

According to the investigation above, it is clear that the toluene/ethanol ratio plays a pivotal role to induce the crystallization of polymer chains into various crystalline forms. To this end, the solvent effect on the formation of crystals is studied in detail. Thus, we turn our attention to elucidate the possible mechanism that results in the formation of different crystals, as illustrated in Figure 7. At a given concentration, the diffusion of polymer chains and the crystal's growth can easily be modulated by the solvent ratio when the crystallization takes place. The process of crystallization includes two steps: the nucleation and the growth of crystals. The addition of ethanol to the toluene solution can affect the primary nucleation. Once the nuclei are formed, they will guide the crystal growth in a specific way in different mixed solutions. During the crystallization, both toluene and ethanol will evaporate, and the composition of the solvent will change accordingly. However, nuclei have already existed in the early stage, and the chains will pack into the crystal surface in a certain fashion due to the mixed solvents with different ratios. When F*n* chains are dissolved in toluene solution (good solvent), the chains have enough time to adjust themselves and favor much more mobility to diffuse along the long axis to form lenticular crystals with the slow evaporation of the solvent. After the injection of ethanol (poor solvent), the solubility parameter of the solvent is changed, and thus polymer chains respond by becoming less solvated. This chain motion acts as a trigger to cause the conformational ordering to generate the short helical structures, which serves as a nucleus to continue the crystallization. Alternatively, the diffusion along the long axis of crystals is inhibited, and chains are prone to grow along the $\pi-\pi$ stacking direction. Under this condition, $\pi-\pi$ interactions dominate the crystal growth to give rise to the fibrous entities. Upon further increase of ethanol, polymer chains transform to regular conformation to minimize polymer−solvent interactions. At the same time, the poor solvent around polymer chains change the interaction between the chains and the substrate, thus leading to the perpendicular alignment of backbones. This allows polymer chains to have more freedom to relax into a more thermodynamically favorable conformation rather than being locked in an unfavorable conformation. Solvent-induced packing leads to chains best described as locally ordered. Once the nuclei are created, they are able to induce the crystallization, and longer rod-like crystals are grown. When the crystallization starts to progress in this way, the interaction of alkyl side chains take over in the process. Thus, under this circumstance, the growth direction is along alkyl side chains.

By and large, the morphology of crystals is very sensitive to the growth conditions. During the crystallization processes, the interplay between polymer chains and the solvent is of primary importance. Depending on the solvent ratio, the morphologies of crystals made of F*n* can be varied from lenticular crystals to fibers, even to rods. According to their different thermal stability[23,43] and ability to bear the electron bombardment, we can draw the conclusion that these crystals are different crystalline forms. At the same time, these crystals exhibit different molecular packing behaviors in the crystal growth.

■ CONCLUSION

In summary, it is possible to map a continuous set of morphologies including lenticular crystals, fibers, and rods by controlling the solvent ratio of toluene/ethanol for F*n*. Lenticular crystals are grown from toluene, where the backbones are along the long axis of the crystal. In the toluene/ethanol ratio of 3:1 solution, helical fibers are prepared,

dx.doi.org/10.1021/jp401261u | J. Phys. Chem. B 2013, 117, 8880−8886

in which polymer chains are perpendicular to the long axis of the crystal. When the toluene/ethanol ratio reaches 1:1, the rod-like crystals are obtained, and polymer chains pack vertical to the substrate with their side chains parallel to the substrate and along the crystal growth direction. This is an important step toward a real control of the arrangement of these polymer chains in a crystal, and the implications for controlling the optical and electrical properties are obviously relevant. In addition, the molecular weight has a certain impact on the morphology of crystals, depending on the specific molecular packing. In the case of lenticular crystals and fibrous crystals, the increment of M_{MS} leads to a decrease of the crystallinity of the samples. By stark contrast, the molecular weight has little impact on the crystallinity of rod-like crystals due to the special molecular packing in these crystals.

AUTHOR INFORMATION

Corresponding Author

*E-mail: yandh@ciac.jl.cn.

Notes

The authors declare no competing financial interest.

ACKNOWLEDGMENTS

This work was financially supported by the National Natural Science Foundation of China (21274146 and 51133007).

REFERENCES

(1) Sirringhaus, H.; Brown, P. J.; Friend, R. H.; Nielsen, M. M.; Bechgaard, K.; Langeveld-Voss, B. M. W.; Spiering, A. J. H.; Janssen, R. A. J.; Meijer, E. W.; Herwing, P.; et al. Two-Dimensional Charge Transport in Self-Organized, High-Mobility Conjugated Polymers. *Nature* **1999**, *401*, 685−688.

(2) de Boer, R. W. I.; Gershenson, M. E.; Morpurgo, A. F.; Podzorov, V. Organic Single-Crystal Field-Effect Transistors. *Phys. Status Solidi A* **2004**, *201*, 1302−1331.

(3) Ong, B. S.; Wu, Y. L.; Liu, P.; Gardner, S. High-Performance Semiconducting Polythiophenes for Organic Thin-Film Transistors. *J. Am. Chem. Soc.* **2004**, *126*, 3378−3379.

(4) Panzer, M. J.; Frisbie, C. D. High Carrier Density and Metallic Conductivity in Poly(3-hexylthiophene) Achieved by Electrostatic Charge Injection. *Adv. Funct. Mater.* **2006**, *16*, 1051−1056.

(5) Li, Y. N.; Sonar, P.; Singh, P. S.; Soh, M. S.; Meurs, M. V.; Tan, J. Annealing-Free High-Mobility Diketopyrrolopyrrole-Quaterthiophene Copolymer for Solution-Processed Organic Thin Film Transistors. *J. Am. Chem. Soc.* **2011**, *113*, 2198−2204.

(6) Li, G.; Zhu, R.; Yang, Y. Polymer Solar Cells. *Nat. Photonics* **2012**, *6*, 153−161.

(7) Dou, L.; You, J. B.; Yang, J.; Chen, C. C.; He, Y. J.; Murase, S.; Moriarty, T.; Emery, K.; Li, G.; Yang, Y. Tandem Polymer Solar Cells Featuring A Spectrally Matched Low-bandgap Polymer. *Nat. Photonics* **2012**, *6*, 180−185.

(8) Sirringhaus, H.; Brown, P. J.; Friend, R. H.; Nielsen, M. M.; Bechgaard, K.; Langeveld-Voss, B. M. W.; Spiering, A. J. H.; Janssen, R. A. J.; Meijer, E. W.; Herwing, P.; Leeuw, D. M. Two-Dimensional Charge Transport in Self-Organized, High-Mobility Conjugated Polymers. *Nature* **1999**, *401*, 685−688.

(9) Majewski, L. A.; Kingsley, J. W.; Balocco, C.; Song, A. M. Influence of Processing Conditions on the Stability of Poly(3-hexylthiophene)-Based Field-Effect Transistors. *Appl. Phys. Lett.* **2006**, *88*, 222108.

(10) Zhang, R.; Li, B.; Iovu, M. C.; Jeffries-EL, M.; Sauve, G.; Cooper, J.; Jia, S. J.; Tristram-Nagle, S.; Smilgies, D. M.; Lambeth, D. N.; McCullough, R. D.; Kowalewski, T. Nanostructure Dependence of Field-Effect Mobility in Regioregular Poly(3-hexylthiophene) Thin Film Field Effect Transistors. *J. Am. Chem. Soc.* **2006**, *128*, 3480−3481.

(11) Chen, S. A.; Lu, H. H.; Huang, C. W. Polyfluorenes for Device Applications. *Adv. Polym. Sci.* **2008**, *212*, 49−84.

(12) Tashiro, K.; Ono, K.; Minagawa, Y.; Kobayashi, M.; Kawai, T.; Yoshino, K. Structure and Thermochromic Solid-State Phase Transition of Poly(3-alkylthiophene). *J. Polym. Sci., Part B: Polym. Phys.* **1991**, *29*, 1223−1233.

(13) Prosa, T. J.; Winokur, M. J.; Moulton, Jeff.; Smith, Paul.; Heeger, A. J. X-ray Structural Studies of Poly(3-alkylthiophenes): An Example of an Inverse Comb. *Macromolecules* **1992**, *25*, 4364−4372.

(14) Meille, S. V.; Romita, V.; Caronna, T.; Lovinger, A. J.; Catellani, M.; Belobrzeckaja, L. Influence of Molecular Weight and Regioregularity on the Polymorphic Behavior of Poly(3-decylthiophenes). *Macromolecules* **1997**, *30*, 7898−7905.

(15) Kim, D. H.; Han, J. T.; Park, Y. D.; Jang, Y.; Cho, J. H.; Hwang, M.; Cho, K. Single-Crystal Polythiophene Microwires Grown by Self-Assembly. *Adv. Mater.* **2006**, *18*, 719−723.

(16) Ma, Z. Y.; Geng, Y. H.; Yan, D. H. Extended-Chain Lamellar Packing of Poly(3-butylthiophene) in Single Crystals. *Polymer* **2007**, *48*, 31−34.

(17) Ma, Z. Y.; Geng, Y. H.; Yan, D. H. Morphology of Head-to-Tail Poly(3-hexylthiophene) Single Crystals from Solution Crystallization. *Chin. J. Polym. Sci.* **2007**, *25*, 43−46.

(18) Lu, G. H.; Li, L. G.; Yang, X. N. Morphology and Crystalline Transition of Poly(3-butylthiophene) Associated with Its Polymorphic Modifications. *Macromolecules* **2008**, *41*, 2062−2070.

(19) Chen, S. H.; Su, A. C.; Chen, S. A. Crystalline Forms and Emission Behavior of Poly(9,9-di-*n*-octyl-2,7-fluorene). *Macromolecules* **2005**, *38*, 379−385.

(20) Chen, S. H.; Su, A. C.; Su, C. H.; Chen, S. A. Phase Behavior of Poly(9,9-di-*n*-hexyl-2,7-fluorene). *J. Phys. Chem. B* **2006**, *110*, 4007−4013.

(21) Liu, C. F.; Wang, Q. L.; Tian, H. K.; Geng, Y. H.; Yan, D. H. Extended-chain Lamellar Crystals of Monodisperse Polyfluorenes. *Polymer* **2013**, *54*, 2459−2465.

(22) Liu, C. F.; Wang, Q. L.; Tian, H. K.; Liu, J.; Geng, Y. H.; Yan, D. H. Morphology and structures of the β Phase Crystals of Monodisperse Polyfluorenes. *Macromolecules* **2013**, *46*, 3025−3030.

(23) Liu, C. F.; Sui, A. G.; Wang, Q. L.; Tian, H. K.; Liu, J.; Geng, Y. H.; Yan, D. H. Fractionated Crystallization of Polydisperse Polyfluorenes. *Polymer* **2013**, *54*, 3150−3155.

(24) Lim, J. A.; Liu, F.; Ferdous, S.; Muthukumar, M.; Briseno, A. L. Polymer Semiconductor Crystals. *Mater. Today* **2010**, *13*, 14−24.

(25) Misaki, M.; Ueda, Y.; Nagamatsu, S.; Chikamatsu, M.; Yoshida, Y.; Tanigaki, N.; Yase, K. Highly Polarized Polymer Light-Emitting Diodes Utilizing Friction-Transferred Poly(9,9-dioctylfluorene) Thin Films. *Appl. Phys. Lett.* **2005**, *87*, 243503.

(26) Greenham, N. C.; Friend, R. H.; Bradley, D. D. C. Angular Dependence of the Emission from a Conjugated Polymer Light-Emitting Diode: Implications for Efficiency Calculations. *Adv. Mater.* **1994**, *6*, 491−494.

(27) Rothe, C.; Galbrecht, F.; Scherf, U.; Monkman, A. The β-Phase of Poly(9,9-dioctylfluorene) as a Potential System for Electrically Pumped Organic Lasing. *Adv. Mater.* **2006**, *18*, 2137−2140.

(28) Kline, R. J.; McGehee, M. D.; Kadnikova, E. N.; Liu, J. S.; Frechet, J. M. J. Controlling the Field-Effect Mobility of Regioregular Polythiophene by Changing the Molecular Weight. *Adv. Mater.* **2003**, *15*, 1519−1522.

(29) Zen, A.; Pflaum, J.; Hirschmann, S.; Zhuang, W.; Jaiser, F.; Asawapirom, U.; Rabe, J. P.; Scherf, U.; Neher, D. Effect of Molecular Weight and Annealing of Poly(3-hexylthiophene)s on the Performance of Organic Field-Effect Transistors. *Adv. Funct. Mater.* **2004**, *14*, 757−764.

(30) Brinnkmann, M.; Rannou, P. Effect of Molecular Weight on the Structure and Morphology of Oriented Thin Films of Regioregular Poly(3-hexylthiophene) Grown by Directional Epitaxial Solidification. *Adv. Funct. Mater.* **2007**, *17*, 101−108.

(31) Grell, M.; Bradley, D. D. C.; Ungar, G.; Hill, J.; Whitehead, K. S. Interplay of Physical Structure and Photophysics for a Liquid Crystalline Polyfluorene. *Macromolecules* **1999**, *32*, 5810−5817.

(32) Chen, S. H.; Chou, H. L.; Su, A. C.; Chen, S. A. Molecular Packing in Crystalline Poly(9,9-di-*n*-octyl-2,7-fluorene). *Macromolecules* **2004**, *37*, 6833−6838.
(33) Knaapila, M.; Dias, F. B.; Garamus, V. M.; Almasy, L.; Torkkeli, M.; Leppanen, K.; Galbrecht, F.; Preis, E.; Burrows, H. D.; Scherf, U.; Monkman, A. P. Influence of Side Chain Length on the Self-Assembly of Hairy-Rod Poly(9,9-dialkylfluorene)s in the Poor Solvent Methylcyclohexane. *Macromolecules* **2007**, *40*, 9398−9405.
(34) Zhou, J. J.; Li, J.; Fu, Y. Q.; Bo, Z. S.; Li, L.; Chan, C. M. Rod-like Crystal Growth of Dioctyl Substituted Polyfluorene from Nematic and Isotropic States. *Polymer* **2007**, *48*, 2503−2507.
(35) Brinkmann, M. Directional Epitaxial Crystallization and Tentative Crystal Structure of Poly(9,9′-di-*n*-octyl-2,7-fluorene). *Macromolecules* **2007**, *40*, 7532−7541.
(36) Knaapila, M.; Winokur, M. J. Structure and Morphology of Polyfluorenes in Solutions and the Solid State. *Adv. Polym. Sci.* **2008**, *212*, 227−272.
(37) Brinkmann, M.; Charoenthai, N.; Traiphol, R.; Piyakulawat, P.; Wlosnewski, J.; Asawapirom, U. Structure and Morphology in Highly Oriented Films of Poly(9,9-bis(*n*-octyl)fluorene-2,7-diyl) and Poly-(9,9-bis(2-ethylhexyl)fluorene-2,7-diyl) Grown on Friction Transferred Poly(tetrafluoroethylene). *Macromolecules* **2009**, *42*, 8298−8306.
(38) Hu, Z. J.; Zhang, F. J.; Huang, H. Y.; Zhang, M. L.; He, T .B. Morphology and Structure of Poly(di-*n*-butylsilane) Single Crystals Prepared by Controlling Kinetic Process of Solvent Evaporation. *Macromolecules* **2004**, *37*, 3310−3318.
(39) Xiao, X. L.; Wang, Z. B.; Hu, Z. J.; He, T. B. Single Crystals of Polythiophene with Different Molecular Conformations Obtained by Tetrahydrofuran Vapor Annealing and Controlling Solvent Evaporation. *J. Phys. Chem. B* **2010**, *114*, 7452−7460.
(40) Brinkmann, M. Structure and Morphology Control in Thin Films of Regioregular Poly(3-hexylthiophene). *J. Polym. Sci., Part B: Polym. Phys.* **2011**, *49*, 1218−1233.
(41) Scharsich, C.; Lohwasser, R. H.; Sommer, M.; Asawapirom, U.; Scherf, U.; Thelakkat, M.; Neher, D.; Kohler, N. Control of Aggregate Formation in Poly(3-hexylthiophene) by Solvent, Molecular Weight, and Synthetic Method. *Polym. Sci., Part B: Polym. Phys.* **2012**, *50*, 442−453.
(42) Shcherbina, M. A.; Chvalun, S. N.; Ungar, G. Effect of Crystallization Conditions on the Shape of Polymer Single Crystals: Experimental and Theoretical Approaches. *Crystallography Reports* **2007**, *52*, 707−720.
(43) Liu, C. F.; Wang, Q. L.; Tian, H. K.; Liu, J.; Geng, Y. H.; Yan, D. H. Insight into Lamellar Crystals of Monodisperse Polyfluorenes-Fractionated Crystallization and the Crystal's Stability. *Polymer* **2013**, *54*, 1251−1258.
(44) Wang, Q. L.; Qu, Y.; Tian, H. K.; Geng, Y. H.; Wang, F. S. Iterative Binomial Synthesis of Monodisperse Polyfluorenes up to 64-mers and Their Chain-Length-Dependent Properties. *Macromolecules* **2011**, *44*, 1256−1260.
(45) Wang, S. H.; Kappl, M.; Liebewirth, I.; Müller, M.; Kirchhoff, K.; Pisula, W.; Müller, K. Organic Field-Effect Transistors based on Highly Ordered Single Polymer Fibers. *Adv. Mater.* **2012**, *24*, 417−420.
(46) Dong, H. L.; Jiang, S. D.; Jiang, L.; Liu, Y. L.; Li, H. X.; Hu, W. P.; Wang, E. J.; Yan, S. K.; Wei, Z. M.; Xu, W.; Gong, X. Nanowire Crystals of a Rigid Rod Conjugated Polymer. *J. Am. Chem. Soc.* **2009**, *131*, 17315−17320.
(47) Yusoff, S. F. M.; Hsiao, M. S.; Schacher, F. H.; Winnik, M. A.; Manners, I. Formation of Lenticular Platelet Micelles via the Interplay of Crystallization and Chain Stretching: Solution Self-Assembly of Poly(ferrocenyldimethylsilane)-block-poly(2-vinylpyridine) with a Crystallizable Core-Forming Metalloblock. *Macromolecules* **2012**, *45*, 3883−3891.
(48) Xiao, X. L.; Hu, Z. J.; Wang, Z. B.; He, T. B. Study on the Single Crystals of Poly(3-octylthiophene) Induced by Solvent-Vapor Annealing. *J. Phys. Chem. B* **2009**, *113*, 14604−14610.
(49) Ihn, K. J.; Moulton, J.; Smith, P. Whiskers of Poly(3-alkylthiophene)s. *J. Polym. Sci., Part B: Polym. Phys.* **1993**, *31*, 735−742.
(50) Leclere, Ph.; Surin, M.; Viville, P.; Lazzaroni, R.; Kilbinger, A. F. M.; Henze, O.; Feast, W. J.; Cavallini, M.; Biscarini, F.; Schenning, A. P. H. J.; Meijer, E. W. About Oligothiophene Self-Assembly: From Aggregation in Solution to Solid-State Nanostructures. *Chem. Mater.* **2004**, *16*, 4452−4466.
(51) Ajayanghosh, A.; Praveen, V. π-Organogels of Self-Assembled *p*-Phenylenevinylenes: Soft Materials with Distinct Size, Shape, and Functions. *Acc. Chem. Res.* **2007**, *40*, 644−656.